



## OPEN Light squeezing enhancement by coupling nonlinear optical cavities

H. Jabri<sup>1</sup>✉ & H. Eleuch<sup>2,3,4</sup>

In this paper, we explore the squeezing effect generated by two coupled optical cavities. Each cavity contains a second-order nonlinear material and coherently pumped by a laser. Our results show that light intensity is strongly improved due to the presence of the nonlinearities and mainly depends on the detunings between external laser frequencies and cavity modes. More interestingly, the proposed scheme could enhance light squeezing for moderate coupling between cavities: the squeezing generated by one cavity is enhanced by the other one. For resonant interaction, highest squeezing effect is obtained near resonance. When fields are non resonant, squeezing increases near resonance of the considered cavity, but decreases for large detunings relative to the second cavity. Further, when the dissipation rate of the second cavity is smaller than the first, the squeezing could be improved, attaining nearly the perfect squeezing. While the temperature elevation has a negative impact overall on the nonclassical light, squeezing shows an appreciable resistance against thermal baths for appropriate parameter sets.

Nonlinear interactions in optical cavities systems are at the origin of the appearance of intriguing phenomena and observations. Starting from optical bistability and multistability<sup>1–3</sup>, several nonclassical features of light have been investigated such as squeezing<sup>4–6</sup>, sub-Poissonian photon statistics<sup>7,8</sup>, antibunching<sup>9–11</sup>, entanglement<sup>12,13</sup>, and Bell nonlocality<sup>14,15</sup>. In quantum optics, one of the field quadratures of squeezed states has smaller fluctuations compared to coherent light or a vacuum. The squeezing property of light is an essential resource in various applications. Not only it is used to reduce the noise level in optical communication<sup>16,17</sup> and for the detection of extremely weak gravitational waves<sup>18,19</sup>, but also in quantum limited displacement sensing<sup>20</sup>, quantum cryptography<sup>21–23</sup> and quantum computing<sup>24–26</sup>. In quantum computing, the reduction of noise below the shot-noise level is used to avoid the loss of encoded information during quantum computation, which could lead to an accumulation of errors. Therefore, by reducing tiny quantum-level fluctuations, scientists have been experimenting with squeezed light to reduce information loss<sup>24</sup>. Furthermore, the most notable application of squeezed light is to increase the astrophysical limits of gravitational-wave detectors including the laser interferometer gravitational-wave observatory (LIGO)<sup>27</sup> and the gravitational-wave observatory (GEO 600) detectors<sup>28</sup>.

Squeezing property of light has been widely investigated in optics. This includes various systems and platforms such as two-level atomic system<sup>29–34</sup>, optomechanical systems<sup>35,36</sup>, quantum well cavity<sup>37–42</sup> and many others. In all cases, the existence of optical nonlinearities, of second or third degree, is needed for the occurrence of the effect. For example, this can be realized by inserting a second-order nonlinear material in a cavity, or by realizing in a quantum well the strong light-matter coupling regime with a high excitonic density. Then, the additional Kerr type nonlinearities that could appear by coupling quantum wells via electronic tunnelling is proved to improve the squeezing effect<sup>40,42</sup>.

In light of this, we propose here a scheme consisting of two coupled cavities containing  $\chi^{(2)}$  materials and we show how this association could enhance the squeezing produced by one cavity and we provide the fundamental system requirements for the effect occurrence. The paper is organized as follows. In section 2 we give the Hamiltonian describing the system and we derive the corresponding evolution equations. Section 3 is consecrated to the study of the intensity of light inside cavities. In section 4, we determine the noise spectrum of the output light and we examine the squeezing property as a function of the frequency detunings, the amplitudes of squeezed light and the coupling strength between the cavities for resonant and off-resonant interactions.

<sup>1</sup>Higher Institute of Biotechnology of Beja, University of Jendouba, Beja 9000, Tunisia. <sup>2</sup>Department of Applied Physics and Astronomy, University of Sharjah, Sharjah 27272, United Arab Emirates. <sup>3</sup>College of Arts and Sciences, Abu Dhabi University, Abu Dhabi 59911, United Arab Emirates. <sup>4</sup>Institute for Quantum Science and Engineering, Texas A&M University, College Station, TX 77843, USA. ✉email: housseem.jabri@isbj.u-jendouba.tn

### Hamiltonian and equations of motion

The hybrid system under investigation, as shown in the schematic representation of Fig. 1, consists of two coupled cavities containing a  $\chi^{(2)}$  material. The cavity A has a frequency  $\omega_a$  and a dissipation rate  $\kappa_1$ , while the frequency of cavity B is  $\omega_b$  and its dissipation rate is  $\kappa_2$ . The pump field of amplitude  $P_{01}$  ( $P_{02}$ ) linearly drives cavity A (B). The pump field  $\varepsilon_1$  drives the crystal of nonlinear susceptibility  $\chi_A^{(2)}$  placed in cavity A, while the crystal inside cavity B, of nonlinear susceptibility  $\chi_B^{(2)}$ , is driven by the pump field  $\varepsilon_2$ . Directly pumping the nonlinear mediums results in a down-conversion process, which is responsible in the creation of highly correlated photon pairs and the appearance of squeezing. The interaction Hamiltonian of the whole system in the rotating wave approximation is given by

$$\begin{aligned}
 H = & -\Delta_1 a_1^\dagger a_1 - \Delta_2 a_2^\dagger a_2 + iJ(a_1^\dagger a_2 - a_2^\dagger a_1) \\
 & + i\frac{\varepsilon_1}{2}(a_1^{\dagger 2} - a_1^2) + i\frac{\varepsilon_2}{2}(a_2^{\dagger 2} - a_2^2) \\
 & + iP_{01}(a_1^\dagger - a_1) + iP_{02}(a_2^\dagger - a_2)
 \end{aligned} \tag{1}$$

where  $a_1^\dagger$  ( $a_2^\dagger$ ) is creation operator of photons in cavity A (cavity B).  $\varepsilon_1 = \chi_A^{(2)} \varepsilon_{pA}$  ( $\varepsilon_2 = \chi_B^{(2)} \varepsilon_{pB}$ ) with  $\varepsilon_{pA}$  ( $\varepsilon_{pB}$ ) being the amplitude of the pump field that drives the crystal. The parameter  $J$  represents the strength of the photon hopping interaction between two cavities.  $\Delta_1 = \omega_{LA} - \omega_a$  ( $\Delta_2 = \omega_{LB} - \omega_b$ ) is frequency detuning between pump laser driving cavity A and cavity A mode (frequency detuning between pump laser driving cavity B and cavity B mode).

The dynamics of the system is governed by the master equation for the density matrix

$$\frac{d\rho}{dt} = -i[H, \rho(t)] + \mathcal{L} \rho(t)^{loss} \tag{2}$$

where  $\mathcal{L}[q] = 2q\rho q^\dagger - \{q^\dagger q, \rho\}$  ( $q \equiv a_1, a_2$ ) is the Lindblad superoperator for photonic dissipations in the two cavities. Then, the dissipative dynamics of the system is described by a set of quantum Langevin equations

$$\frac{da_1}{dt} = \left(i\Delta_1 - \frac{\kappa_1}{2}\right)a_1 + Ja_2 + \varepsilon_1 a_1^\dagger + P_{01} + \sqrt{\kappa_1} a_1^{in} \tag{3}$$

$$\frac{da_2}{dt} = \left(i\Delta_2 - \frac{\kappa_2}{2}\right)a_2 - Ja_1 + \varepsilon_2 a_2^\dagger + P_{02} + \sqrt{\kappa_2} a_2^{in} \tag{4}$$

We assume that the cavity modes, relative to cavity A and B, are coupled to thermal reservoirs and the noise operators are  $\delta$  correlated:

$$\langle a_1^{in}(t) a_1^{in\dagger}(t') \rangle = (n_{a1} + 1) \delta(t - t') \tag{5}$$

$$\langle a_1^{in\dagger}(t) a_1^{in}(t') \rangle = n_{a1} \delta(t - t') \tag{6}$$

for cavity A, and

$$\langle a_2^{in}(t) a_2^{in\dagger}(t') \rangle = (n_{a2} + 1) \delta(t - t') \tag{7}$$

$$\langle a_2^{in\dagger}(t) a_2^{in}(t') \rangle = n_{a2} \delta(t - t') \tag{8}$$

for cavity B, where  $n_{a1}$  and  $n_{a2}$  are the mean numbers of thermal photons in each cavity.

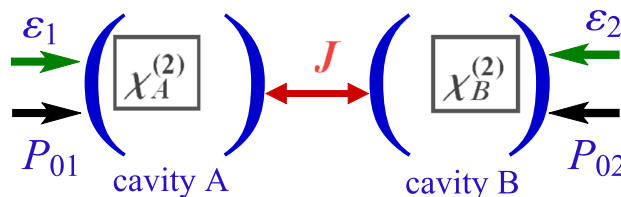


**Figure 1.** Two coupled cavities containing an optical parametric oscillator that generates a second-order optical nonlinearity. The resulting squeezed light from the nonlinear process in a cavity can be transferred to the other one. Cavity A (B) is pumped by a laser with an amplitude  $P_{01}$  ( $P_{02}$ ) with a decay rate  $\kappa_1$  ( $\kappa_2$ ).

### Light intensity

Here, we study the intensity of light inside the cavities. However, as the difference between cavity A and cavity B is only the difference in system parameters, then by studying cavity A also implies studying cavity B. In the following, we consider cavity A which is applicable to cavity B. The evolution equations of the mean photon numbers are deduced from Eqs. (3) and (4) by removing the fluctuation terms

$$\frac{d\bar{a}_1}{dt} = \left(i\Delta_1 - \frac{\kappa_1}{2}\right)\bar{a}_1 + J\bar{a}_2 + \varepsilon_1\bar{a}_1^\dagger + P_{01} \tag{9}$$

$$\frac{d\bar{a}_2}{dt} = \left(i\Delta_2 - \frac{\kappa_2}{2}\right)\bar{a}_2 - J\bar{a}_1 + \varepsilon_2\bar{a}_2^\dagger + P_{02} \tag{10}$$

Eqs. (9) and (10) are similar with the temporal coupled-mode theory used in Refs.<sup>43,44</sup>. After solving these equations in the steady-state regime and considering the case of  $\kappa_1 = \kappa_2 = \kappa$ , we plot in Fig. 2a the light intensity of cavity A,  $|\bar{a}_1|^2$ , as a function of the detuning  $\Delta/\kappa$  where we assume that  $\Delta_1 = \Delta_2 = \Delta$ . It can be seen that for  $J = 0$ , meaning that cavity B is decoupled from cavity A, maximal intensity appears at resonance ( $\Delta = 0$ ) as a single peak, i.e., when the coherent driving field is at resonance with the cavity radiation frequency for cavity A. When cavity B is introduced with a photon interaction strength  $J = \kappa$  and an amplitude of the pump field driving the crystal (which is directly linked to the degree of squeezing)  $\varepsilon_2 = 0.2\kappa$ , we observe that photonic intensity increases considerably and the spectrum has two peaks of same width centered around  $\Delta = \pm J$ . The distance separating the intensity peaks increases as the interaction is increased. This is noticed when  $J = 3\kappa$ .

Now, we extend our study to non-resonant interactions ( $\Delta_1 \neq \Delta_2$ ). The density plot of Fig. 2b shows that the intensity has two branches of light. Away from this, the number of photons in the cavity is highly reduced. It is interesting to highlight that maximal intensity is obtained near resonance of cavity A, but away from resonance for cavity B.

Light intensity study is important in the measure that it provides the general conditions to obtain a non zero or maximal photon number in the cavity. This will guide us to find the system parameters for optimal degree of squeezing which will be discussed in the following section.

### Squeezing spectrum of the output light from cavity A

To determine the noise spectrum of the output field, it is more convenient to write the operators  $a_1$  and  $a_2$  that appear in Eqs. (3) and (4) as the sum of mean field values and fluctuations operators, as  $a_1(t) = \bar{a}_1 + \delta a_1(t)$  and  $a_2(t) = \bar{a}_2 + \delta a_2(t)$ . The fluctuation parts  $\delta a_1$  and  $\delta a_2$  are supposed to be very small compared to the mean values  $\bar{a}_1$  and  $\bar{a}_2$ . Then, the fluctuations satisfy the following equations

$$\frac{d}{dt}\delta a_1 = \left(i\Delta_1 - \frac{\kappa_1}{2}\right)\delta a_1 + J\delta a_2 + \varepsilon_1\delta a_1^\dagger + \sqrt{\kappa_1}a_1^{in} \tag{11}$$

$$\frac{d}{dt}\delta a_2 = \left(i\Delta_2 - \frac{\kappa_2}{2}\right)\delta a_2 - J\delta a_1 + \varepsilon_2\delta a_2^\dagger + \sqrt{\kappa_2}a_2^{in} \tag{12}$$

The phenomenon of squeezing occurs when a field quadrature has a lower noise than coherent light. As we are interested in optical field statistics of cavity A, it can be defined, by the general relationship, for a quadrature  $A_\theta = a_1^\dagger e^{i\theta} + a_1 e^{-i\theta}$

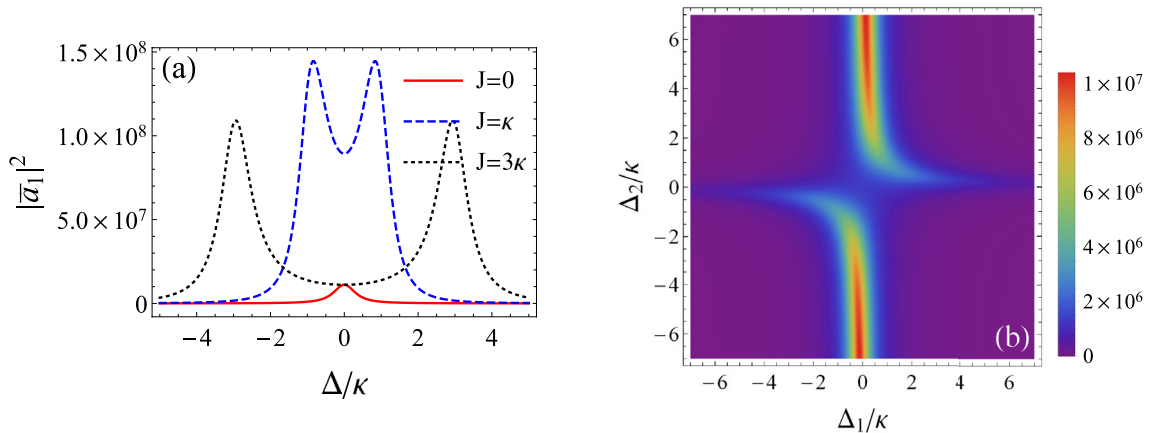


**Figure 2.** (a) mean photon number of cavity A as a function of the detuning  $\Delta/\kappa$  for various couplings  $J$ . The parameters are  $P_{01} = 10^3\kappa$ ,  $P_{02} = 10^4\kappa$  and  $\varepsilon_1 = \varepsilon_2 = 0.2\kappa$ . (b) density plot of the photon mean number versus the detunings  $\Delta_1$  and  $\Delta_2$  for  $J = \kappa$ ,  $P_{01} = P_{02} = 10^3\kappa$ ,  $\varepsilon_1 = 0.2\kappa$  and  $\varepsilon_2 = 0.25\kappa$ .

$$\begin{aligned}
 S_\theta(\omega) &= \int_{-\infty}^{+\infty} \langle A_\theta(t); A_\theta(0) \rangle e^{-i\omega t} dt \\
 &= \int_{-\infty}^{+\infty} C_{A_\theta A_\theta} e^{-i\omega t} dt
 \end{aligned}
 \tag{13}$$

where  $\theta$  is the field phase angle and  $C_{A_\theta A_\theta}$  is the covariance of the quadrature  $A_\theta$  defined by

$$\begin{aligned}
 C_{A_\theta A_\theta}(t) &= \langle A_\theta(t); A_\theta(0) \rangle \\
 &= \langle A_\theta(t) A_\theta(0) \rangle - \langle A_\theta(t) \rangle \langle A_\theta(0) \rangle
 \end{aligned}
 \tag{14}$$

By writing the quadrature operator  $A_\theta$  as the sum of a mean value and a fluctuation term,  $A_\theta = \bar{A}_\theta + \delta A_\theta$ , the covariance function  $C_{A_\theta A_\theta}$  is interpreted as the average of the product of the fluctuations  $\delta A_\theta$  at two instants separated by a time lapse  $t$ :  $C_{A_\theta A_\theta} = \langle \delta A_\theta(t) \delta A_\theta(0) \rangle$ . Then, the noise spectrum  $S_\theta(\omega)$  represents the Fourier transform of the covariance  $C_{A_\theta A_\theta}$

$$S_\theta(\omega) = \int_{-\infty}^{+\infty} \langle \delta A_\theta(t) \delta A_\theta(0) \rangle e^{-i\omega t} dt
 \tag{15}$$

where, here,  $\delta A_\theta$  represents a quadrature of the field relative to the fluctuation operators defined by  $\delta A_\theta = e^{-i\theta} \delta a_1 + e^{i\theta} \delta a_1^\dagger$ . Working in the frequency domain makes the coupled differential equations given by Eqs. (11) and (12) simpler. Additionally, experimentally, the electric field fluctuations are more convenient to measure in the frequency domain than in the time domain. Indeed, the squeezing spectra can be easily measured in the outgoing light using a radiofrequency spectrum analyser connected to photodetectors. These spectra are directly related to the solutions of the linearized equations in the frequency domain  $\delta a_1^{out}(\omega)$  and  $\delta a_1^{out\dagger}(\omega)$ . In fact, experiments allow us to measure the fluctuations of the output electric field in a quadrature defined by an angle  $\theta$  with respect to some phase reference:  $\delta A_\theta^{out}(\omega) = e^{-i\theta} \delta a_1^{out}(\omega) + e^{i\theta} \delta a_1^{out\dagger}(\omega)$ , and the measured spectra are given by  $\langle \delta A_\theta^{out}(\omega) \delta A_\theta^{out}(\omega) \rangle$ <sup>45,46</sup>. Given this, the noise spectrum  $S_\theta(\omega)$  is thus written as

$$\begin{aligned}
 S_\theta(\omega) &= 1 + 2C_{a_1^\dagger a_1}(\omega) + C_{a_1 a_1}(\omega) e^{-2i\theta} \\
 &\quad + C_{a_1^\dagger a_1}(\omega) e^{2i\theta}
 \end{aligned}
 \tag{16}$$

The correlation function  $C_{a_1^\dagger a_1}(\omega)$  is defined by  $\langle \delta a_1^\dagger(\omega) \delta a_1(\omega') \rangle = 2\pi \delta(\omega + \omega') C_{a_1^\dagger a_1}(\omega)$ . The other correlations are defined in a similar way.

The noise spectrum of vacuum or a coherent state is independent of frequency and quadrature angle  $\theta$ , it is always equal to 1 and this corresponds to the shot noise or the standard quantum noise,  $(S_\theta(\omega))_{shot} = 1$ . A field is said to be squeezed if one of its quadratures has fluctuations in which one of the frequency components has a noise lower than standard quantum noise, meaning if there exist  $\theta$  and  $\omega$  such as  $S_\theta(\omega) < 1$ . The optimized noise spectrum corresponds to the value of  $\theta$  which maximizes the squeezing. By solving the equation  $dS_\theta(\omega)/d\theta = 0$ , the angle  $\theta$  satisfies the relation  $e^{2i\theta_{opt}} = \pm C_{a_1 a_1} / |C_{a_1 a_1}|$ . Then, the optimized squeezing spectrum of the emergent light is given by<sup>47</sup>

$$S_{opt}(\omega) = 1 + 2 \left[ C_{a_1^\dagger a_1}(\omega) - |C_{a_1 a_1}(\omega)| \right].
 \tag{17}$$

The set of equations (11), (12) can be rewritten in simpler form as:  $\mathcal{A} \cdot \mathcal{U} = \mathcal{N}$ , where

$$\mathcal{A} = \begin{pmatrix} \alpha_- & -J & -\varepsilon_1 & 0 \\ J & \beta_- & 0 & -\varepsilon_2 \\ -\varepsilon_1 & 0 & \alpha_+ & -J \\ 0 & -\varepsilon_2 & J & \beta_+ \end{pmatrix}
 \tag{18}$$

with  $\alpha_\mp = i\omega \mp i\Delta_1 + \frac{\kappa_1}{2}$  and  $\beta_\mp = i\omega \mp i\Delta_2 + \frac{\kappa_2}{2}$ , and

$$\mathcal{U} = \begin{pmatrix} \delta a_1(\omega) \\ \delta a_2(\omega) \\ \delta a_1^\dagger(\omega) \\ \delta a_2^\dagger(\omega) \end{pmatrix}, \quad \mathcal{N} = \begin{pmatrix} \sqrt{\kappa_1} \delta a_1^{in} \\ \sqrt{\kappa_2} \delta a_2^{in} \\ \sqrt{\kappa_1} \delta a_1^{in\dagger} \\ \sqrt{\kappa_2} \delta a_2^{in\dagger} \end{pmatrix}
 \tag{19}$$

The general solution for the photonic field of cavity A is simply a linear combination of the fluctuations given by:

$$\begin{aligned}
 \delta a_1(\omega) &= \sqrt{\kappa_1} L_1(\omega) a_1^{in} + \sqrt{\kappa_2} L_2(\omega) a_2^{in} \\
 &\quad + \sqrt{\kappa_1} L_3(\omega) a_1^{in\dagger} + \sqrt{\kappa_2} L_4(\omega) a_2^{in\dagger}
 \end{aligned}
 \tag{20}$$

where the  $L_i(\omega)$  ( $i = 1, 2, 3, 4$ ) functions are the elements of the inverse of the matrix  $\mathcal{A}$ , and written as:

$$L_1(\omega) = \mathcal{D}^{-1} [\alpha_+ \beta_- \beta_+ - \alpha_+ \varepsilon_2^2 + \beta_- J^2]
 \tag{21}$$

$$L_2(\omega) = \mathcal{D}^{-1} [J^3 + \alpha_+ \beta_+ J + \varepsilon_1 \varepsilon_2 J]
 \tag{22}$$

$$L_3(\omega) = \mathcal{D}^{-1} [\beta_- \beta_+ \varepsilon_1 - \varepsilon_1 \varepsilon_2^2 - \varepsilon_2 J^2] \quad (23)$$

$$L_4(\omega) = \mathcal{D}^{-1} [\alpha_+ \varepsilon_2 J + \beta_- \varepsilon_1 J] \quad (24)$$

and  $\mathcal{D} = \det(\mathcal{A})$  is given by

$$\begin{aligned} \mathcal{D} = & J^4 + \alpha_- \alpha_+ \beta_- \beta_+ - \alpha_- \alpha_+ \varepsilon_2^2 - \beta_- \beta_+ \varepsilon_1^2 \\ & + \varepsilon_1^2 \varepsilon_2^2 + \alpha_- \beta_- J^2 + \alpha_+ \beta_+ J^2 + 2\varepsilon_1 \varepsilon_2 J^2 \end{aligned} \quad (25)$$

Using Eq. (20) and its complex conjugate, and the input-output relations linking the intracavity and the extracavity fields ( $\delta a_1^{out} = \sqrt{\kappa_1} \delta a - a^{in}$  and  $\delta a_1^{\dagger out} = \sqrt{\kappa_1} \delta a^\dagger - a^{\dagger in}$ ), then the expressions of the extracavity correlation functions are given by

$$\begin{aligned} C_{a^\dagger a}^{out}(\omega) = & \kappa_1 \left[ \kappa_1 n_{a1} |L_1(-\omega)|^2 + \kappa_1 (n_{a1} + 1) |L_3(-\omega)|^2 \right. \\ & \left. + \kappa_2 n_{a2} |L_2(-\omega)|^2 + \kappa_2 (n_{a2} + 1) |L_4(-\omega)|^2 \right] \\ & - 2n_{a1} \kappa_1 \text{Re}[L_1(-\omega)] + n_{a1} \end{aligned} \quad (26)$$

$$\begin{aligned} C_{aa}^{out}(\omega) = & \kappa_1 \left[ \kappa_1 (n_{a1} + 1) L_1(\omega) L_3(-\omega) \right. \\ & \left. + \kappa_2 (n_{a2} + 1) L_2(\omega) L_4(-\omega) \right. \\ & \left. + \kappa_1 n_{a1} L_3(\omega) L_1(-\omega) + \kappa_2 n_{a2} L_4(\omega) L_2(-\omega) \right] \\ & - \kappa_1 n_{a1} L_3(\omega) - \kappa_1 (n_{a1} + 1) L_3(-\omega) \end{aligned} \quad (27)$$

### Light squeezing enhancement

Note that the squeezing spectrum calculated above depends on the parametric down-conversion processes in cavity A and cavity B. These processes are manifested through parameters  $\varepsilon_1$  and  $\varepsilon_2$ , respectively. In this section we analyze the squeezing properties of the emergent light from cavity A as a function of these nonlinearities as well as the mean photon numbers of thermal baths. First, we assume low temperature of the system, when phonon processes are suppressed, and we consider resonant case  $\Delta_1 = \Delta_2 = \Delta$ . The behavior of the squeezing spectrum is shown in Fig. 3a as a function of the detuning  $\Delta/\kappa$  and the frequency  $\omega/\kappa$ . Parameters are such that squeezing strength in cavity A is  $\varepsilon_1 = 0.1\kappa$ , photon hopping interaction strength is  $J = \kappa$  and  $\varepsilon_2 = 0$ . We observe that emerging squeezing appears in four symmetrical peaks with respect to  $\Delta = 0$  and  $\omega = 0$ . The nonclassical effect degree is of 20%. As we go away from these peaks, squeezing decreases and vanishes progressively when  $S_{opt}(\omega) = 1$ , indicating a coherent light. Note here that cavity B contains a mixture of coherent, thermal and squeezed light. By choosing  $\varepsilon_2 = 0$  and  $n_a = n_b = 0$ , photons coming from cavity B are only coherent. Now, we take  $\varepsilon_2 = 0.1\kappa$ . As shown in Fig. 3(b), squeezing is enhanced and reaches 30%. The effect appears mainly in two peaks and remains localized around resonance.

The effect of cavity B on the squeezed radiation of cavity A should be seen more closer. Indeed, Fig. 3c shows a density plot of the noise spectrum  $S_{opt}(\omega)$  against the interaction parameter  $J/\kappa$  and  $\varepsilon_2$ . It is clearly observed that the presence of cavity B strongly improves the squeezing generated by cavity A. The squeezing jumps from nearly 20%, when the cavities are decoupled ( $J = 0$ ), to more than 50%. This is possible for a coupling comparable to the cavity damping rate,  $J \simeq \kappa$ , and a squeezing strength from cavity B of  $\varepsilon_2 = 0.4\kappa$ . However, a stronger cavity couplings does not automatically generate higher squeezing. Thus, for  $J = 2\kappa$  for example, squeezing could disappear even in the presence of the two squeezed sources. Additionally, the coupling to the thermal baths has a negative effect on the squeezed radiation. Fig. 3d illustrates the noise spectrum versus  $\Delta/\kappa$  for different thermal photon mean numbers. It can be seen that as the temperature increases, the nonclassical effect magnitude decreases and fluctuations appear above the shot noise level. Nevertheless, squeezing remains robust around resonance and shows a good resistance.

Now, we consider off-resonant interactions and we plot in Fig. 4 the noise spectrum against the detunings  $\Delta_1/\kappa$  and  $\Delta_2/\kappa$ . If there is no squeezed photons coming from cavity B, the squeezing degree produced by cavity A is of 35% when  $\varepsilon_1 = 0.2\kappa$ . Here, we can observe that there is a region around resonance corresponding to  $\Delta_2 \simeq \pm\kappa$  where squeezing could decrease. This behavior is attributed to the decrease of the light intensity in the cavity around these frequencies as shown in Fig. 2b. Except this, squeezing is obtained for wide ranges of the detuning  $\Delta_2$ . Then,  $\Delta_2$  has a significant influence on the total squeezed radiation. Indeed, the increase of the detuning in cavity B could increase the squeezing in cavity A, as illustrated by the comparative plot of Fig. 4b. Then, the highest squeezing magnitude is obtained close to the resonance and also for large detunings relative to cavity B. This can be explained again based on the behavior of the light intensity which is important near resonance for cavity A and for high detunings for cavity B (Fig. 2b).

The situation changes by injecting squeezed photons from cavity B ( $\varepsilon_2 = 0.25\kappa$ ). Indeed, we note a good enhancement of squeezing especially at resonance reaching more than 70%, meaning an increase of almost 35%

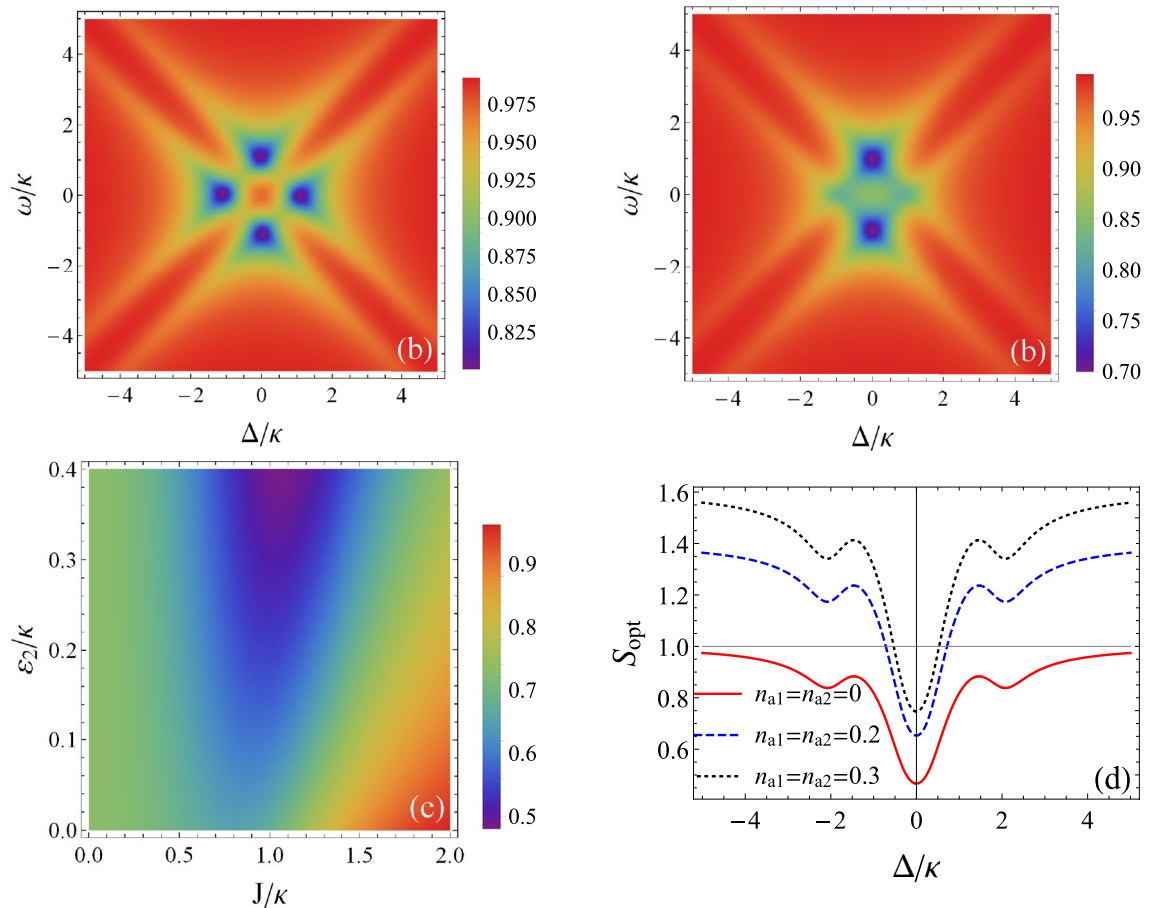


**Figure 3.** Noise spectrum of the output light as a function of the detuning  $\Delta/\kappa$  and the frequency  $\omega/\kappa$  for  $J = \kappa$ ,  $\varepsilon_1 = 0.1\kappa$  and  $n_{a1} = n_{a2} = 0$ : (a)  $\varepsilon_2 = 0$ . (b)  $\varepsilon_2 = 0.1\kappa$ . (c) noise spectrum against the coupling  $J/\kappa$  and the squeezed light amplitude of cavity B  $\varepsilon_2/\kappa$  for  $\Delta = 0$ ,  $\omega = \kappa$ ,  $\varepsilon_1 = 0.2\kappa$  and  $n_{a1} = n_{a2} = 0$ . (d) Noise spectrum against the detuning  $\Delta/\kappa$  for various thermal photon mean numbers, for  $J = \kappa$ ,  $\omega = \kappa$  and  $\varepsilon_1 = \varepsilon_2 = 0.3\kappa$ .

compared to the previous case (Fig. 4c). Here, highest squeezing is localized close to the resonance. Additionally, we notice that the choice of high detunings in cavity B will decrease the squeezing in cavity A (Fig. 4d).

Finally, we consider that the two cavities have different dissipation rates. The system parameters are now scaled to the damping rate of cavity A,  $\kappa_1$ . We observe that when  $\kappa_2$  is greater than  $\kappa_1$ , the squeezing decreases compared to the case of identical cavities. However, if  $\kappa_2$  is smaller than  $\kappa_1$ , the squeezing increases considerably and we could attain an amount of squeezing of 98%, approaching the perfect squeezing, when  $\kappa_2 = 0.66\kappa_1$  (Fig. 4e). Indeed, when cavity B has smaller damping rate, the system is more decoupled from the environment. Then, the nonclassical effect will be more protected inside cavity B. In this case, the coupling between cavity A and cavity B enhances the squeezing of radiated light from cavity A. We also observe that the squeezing is unnoticeably affected by the temperature near the resonance for appropriate parameters sets (Fig. 4f).

## Conclusion

We investigated the squeezing of light produced by two coupled optical cavities containing second-order nonlinear crystals. We have shown that the coupling with a second cavity highly increases the photon intensity in the first cavity, and that light intensity is governed by the frequency detunings of both cavities. Indeed, to observe maximal light we should turn a cavity near resonance and the other away from resonance. We have shown also that the association of two nonlinear cavities could greatly enhance the squeezing compared to the single cavity case. The highest squeezing degree is obtained in a region approaching the resonance for both cavities. When the damping rate of the second cavity is smaller than the first, the squeezing is improved, attaining nearly the perfect squeezing.

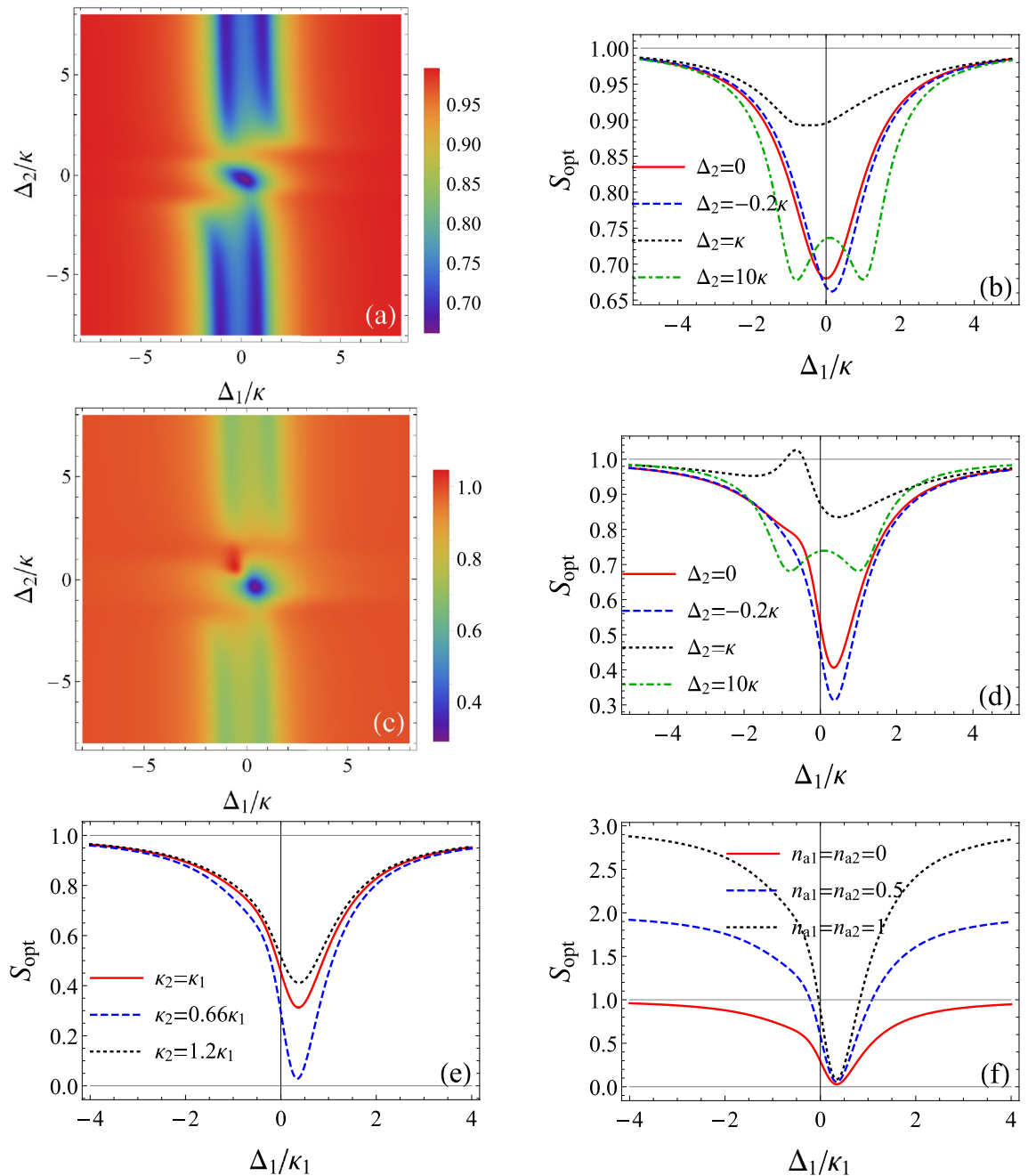


**Figure 4.** Noise spectrum of the output light as a function of the detunings  $\Delta_1/\kappa$  and  $\Delta_2/\kappa$  relative to cavity A and cavity B respectively for  $J = \kappa$ ,  $\varepsilon_1 = 0.2\kappa$ ,  $\omega = \kappa$  and  $n_{a1} = n_{a2} = 0$ : (a) and (b)  $\varepsilon_2 = 0$ . (c) and (d)  $\varepsilon_2 = 0.25\kappa$ . (b) and (d) are comparative plots for different detunings  $\Delta_2$  corresponding to Figs. (a) and (c), respectively. (e) noise spectrum of the output light as a function of the detunings  $\Delta_1/\kappa_1$  for  $J = \kappa_1$ ,  $\varepsilon_1 = 0.2\kappa_1$ ,  $\varepsilon_2 = 0.25\kappa_1$ ,  $\Delta_2 = -0.2\kappa_1$ ,  $\omega = \kappa_1$  and  $n_{a1} = n_{a2} = 0$ . (f) noise spectrum of the output light as a function of the detunings  $\Delta_1/\kappa_1$  for various thermal photon mean numbers and  $\kappa_2 = 0.66\kappa_1$ . The other parameters are the same as (e).

### Data availability

The datasets used and/or analysed during the current study available from the corresponding author on reasonable request. Results are generated using our analytical expressions in the manuscript with defined parameters.

Received: 17 January 2024; Accepted: 29 March 2024

Published online: 02 April 2024

### References

1. Suzhen, Zhang, Li Jiahua, Yu., Rong, Wang Wei & Ying, Wu. Optical multistability and Fano line-shape control via mode coupling in whispering-gallery-mode microresonator optomechanics. *Sci. Rep.* 7, 39781 (2017).

2. Landa, H., Schiró, M. & Misguich, G. Multistability of driven-dissipative quantum spins. *Phys. Rev. Lett.* **124**, 043601 (2020).
3. Jabri, H. & Eleuch, H. Optical bistability and multistability with coupled quantum wells in the presence of second- and third-order nonlinearities. *Chaos, Solitons Fractals* **177**, 114270 (2023).
4. Walls, D. F. Squeezed states of light. *Nature (London)* **306**, 141 (1983).
5. Dodonov, V. 'Nonclassical' states in quantum optics: A 'squeezed' review of the first 75 years. *J. Opt. B* **4**, R1 (2002).
6. Andersen, Ulrik L., Gehring, Tobias, Marquardt, Christoph & Leuchs, Gerd. 30 years of squeezed light generation. *Phys. Scr.* **91**, 053001 (2016).
7. Mandel, L. Sub-Poissonian photon statistics in resonance fluorescence. *Opt. Lett.* **4**, 205–207 (1979).
8. Wang, Y., Ye, H., Yu, Z., Liu, Yumin & Xu, W. Sub-Poissonian photon statistics in quantum dot-metal nanoparticles hybrid system with gain media. *Sci. Rep.* **9**, 10088 (2019).
9. Knight, P. Observation of photon antibunching. *Nature* **269**, 647 (1977).
10. Paul, H. Photon antibunching. *Rev. Mod. Phys.* **54**, 1061 (1982).
11. Lv, B. *et al.* Photon antibunching in a cluster of giant CdSe/CdS nanocrystals. *Nat. Commun.* **9**, 1536 (2018).
12. Kim, M. S., Son, W., Buzek, V. & Knight, P. L. Entanglement by a beam splitter: Nonclassicality as a prerequisite for entanglement. *Phys. Rev. A* **65**, 032323 (2002).
13. Ye, G. S. *et al.* A photonic entanglement filter with Rydberg atoms. *Nat. Photon.* **17**, 538–543 (2023).
14. Brunner, N., Cavalcanti, D., Pironio, S., Scarani, V. & Wehner, S. Bell nonlocality. *Rev. Mod. Phys.* **86**, 419 (2014).
15. Chen, J. L., Ren, C., Chen, C., Ye, X. J. & Pati, A. K. Bell's nonlocality can be detected by the violation of Einstein-Podolsky-Rosen steering inequality. *Sci. Rep.* **6**, 39063 (2016).
16. Yamamoto, Y. & Haus, H. A. Preparation, measurement and information capacity of optical quantum states. *Rev. Mod. Phys.* **58**, 1001–1020 (1986).
17. Suleiman, I. *et al.* 40 km fiber transmission of squeezed light measured with a real local oscillator. *Quantum Sci. Technol.* **7**, 045003 (2022).
18. Zhao, Y. *et al.* Frequency-dependent squeezed vacuum source for broadband quantum noise reduction in advanced gravitational-wave detectors. *Phys. Rev. Lett.* **124**, 171101 (2020).
19. McCuller, L. *et al.* Frequency-dependent squeezing for advanced LIGO. *Phys. Rev. Lett.* **124**, 171102 (2020).
20. Hoff, Ulrich B. *et al.* Quantum-enhanced micromechanical displacement sensitivity. *Opt. Lett.* **38**, 1413–1415 (2013).
21. Hillery, M. Quantum cryptography with squeezed states. *Phys. Rev. A* **61**, 022309 (2000).
22. Gottesman, D. & Preskill, J. Secure quantum key distribution using squeezed states. *Phys. Rev. A* **63**, 022309 (2001).
23. Gisin, N., Ribordy, G., Tittel, W. & Zbinden, H. Quantum cryptography. *Rev. Mod. Phys.* **74**, 145 (2002).
24. Fukui, K., Tomita, A., Okamoto, A. & Fujii, K. High-threshold fault-tolerant quantum computation with analog quantum error correction. *Phys. Rev. X* **8**, 021054 (2018).
25. Douce, T. *et al.* Continuous-variable instantaneous quantum computing is hard to sample. *Phys. Rev. Lett.* **118**, 070503 (2017).
26. Arrazola, J. M. *et al.* Quantum circuits with many photons on a programmable nanophotonic chip. *Nature (London)* **591**, 54 (2021).
27. Aasi, J. *et al.* Enhanced sensitivity of the LIGO gravitational wave detector by using squeezed states of light. *Nat. Photon.* **7**, 613 (2013).
28. Grote, H. *et al.* First long-term application of squeezed states of light in a gravitational-wave observatory. *Phys. Rev. Lett.* **110**, 181101 (2013).
29. Johnsson, M. T. & Haine, S. A. Generating quadrature squeezing in an atom laser through self-interaction. *Phys. Rev. Lett.* **99**, 010401 (2007).
30. Schulte, C. H. H. *et al.* Quadrature squeezed photons from a two-level system. *Nature (London)* **525**, 222 (2015).
31. El-Ella, H. A. R. Driven quadrature and spin squeezing in a cavity-coupled ensemble of two-level states. *Phys. Rev. A* **103**, 023701 (2021).
32. Scholl, P. *et al.* Microwave engineering of programmable XXZ Hamiltonians in arrays of Rydberg atoms. *PRX Quantum* **3**, 020303 (2022).
33. Govia, L. C. G., Lingenfelter, A. & Clerk, A. A. Stabilizing two-qubit entanglement by mimicking a squeezed environment. *Phys. Rev. Res.* **4**, 023010 (2022).
34. Jabri, H. & Eleuch, H. Enhanced unconventional photon-blockade effect in one- and two-qubit cavities interacting with nonclassical light. *Phys. Rev. A* **106**, 023704 (2022).
35. Brooks, Daniel W. C. *et al.* Non-classical light generated by quantum-noise-driven cavity optomechanics. *Nature* **488**, 476–480 (2012).
36. Jabri, H. & Eleuch, H. Squeezed vacuum interaction with an optomechanical cavity containing a quantum well. *Sci. Rep.* **12**, 3658 (2022).
37. Vahala, K. *Optical Microcavities* (World Scientific, 2004).
38. Deveaud, B. *The Physics of Semiconductor Microcavities* (Wiley, 2007).
39. Karr, J. P., Baas, A., Houdre, R. & Giacobino, E. Squeezing in semiconductor microcavities in the strong-coupling regime. *Phys. Rev. A* **69**, 031802(R) (2004).
40. Jabri, H. & Eleuch, H. Quantum noise and squeezed light by dipolaritons in the nonlinear regime. *Ann. Phys.* **531**, 1900253 (2019).
41. Jabri, H. & Eleuch, H. Interaction of a dipolariton system with squeezed light from a parametric down-conversion process. *Phys. Rev. A* **101**, 053819 (2020).
42. Jabri, H. & Eleuch, H. Optical Kerr nonlinearity in quantum-well microcavities: From polariton to dipolariton. *Phys. Rev. A* **102**, 063713 (2020).
43. Hou, Jiankun *et al.* Self-induced transparency in a perfectly absorbing chiral second-harmonic generator. *Photonix* **3**, 22 (2022).
44. Hou, Jiankun, Zhu, Jiefu, Ma, Ruixin, Xue, Boyi, Zhu, Yicheng, Lin, Jintian, Jiang, Xiaoshun, Zheng, Yuanlin, Chen, Xianfeng, Cheng, Ya, Ge, Li, & Wan, Wenjie. Enhanced Frequency Conversion in Parity-Time Symmetry Line. [arXiv:2402.06200](https://arxiv.org/abs/2402.06200).
45. Messin, G., Karr, J. P., Eleuch, H., Courty, J. M. & Giacobino, E. Squeezed states and the quantum noise of light in semiconductor microcavities. *J. Phys. Condens. Matter* **11**, 6069–6078 (1999).
46. Giacobino, E., Karr, J. P., Messin, G., Eleuch, H. & Baas, A. Quantum optical effects in semiconductor microcavities. *C. R. Physique* **3**, 41–52 (2002).
47. Helico, L., Fabre, C., Reynaud, S. & Giacobino, E. Linear input-output method for quantum fluctuations in optical bistability with two-level atoms. *Phys. Rev. A* **46**, 4397–4405 (1992).

## Author contributions

H. J. conceived the idea, performed the mathematical calculations, prepared the presented results, and wrote the original draft. H. E. reviewed and validated the obtained results.

## Competing interests

The authors declare no competing interests.



### Additional information

**Correspondence** and requests for materials should be addressed to H.J.

**Reprints and permissions information** is available at [www.nature.com/reprints](http://www.nature.com/reprints).

**Publisher's note** Springer Nature remains neutral with regard to jurisdictional claims in published maps and institutional affiliations.



**Open Access** This article is licensed under a Creative Commons Attribution 4.0 International License, which permits use, sharing, adaptation, distribution and reproduction in any medium or format, as long as you give appropriate credit to the original author(s) and the source, provide a link to the Creative Commons licence, and indicate if changes were made. The images or other third party material in this article are included in the article's Creative Commons licence, unless indicated otherwise in a credit line to the material. If material is not included in the article's Creative Commons licence and your intended use is not permitted by statutory regulation or exceeds the permitted use, you will need to obtain permission directly from the copyright holder. To view a copy of this licence, visit <http://creativecommons.org/licenses/by/4.0/>.

© The Author(s) 2024